

# Time evolution of the chiral phase transition during a spherical expansion

Melissa A. Lampert\* and John F. Dawson†

*Department of Physics  
University of New Hampshire  
Durham, NH 03824, USA*

Fred Cooper‡

*Theoretical Division  
Los Alamos National Laboratory  
Los Alamos, NM 87545, USA  
(November 15, 2021)*

We examine the non-equilibrium time evolution of the hadronic plasma produced in a relativistic heavy ion collision, assuming a spherical expansion into the vacuum. We study the  $O(4)$  linear sigma model to leading order in a large- $N$  expansion. Starting at a temperature above the phase transition, the system expands and cools, finally settling into the broken symmetry vacuum state. We consider the proper time evolution of the effective pion mass, the order parameter  $\langle\sigma\rangle$ , and the particle number distribution. We examine several different initial conditions and look for instabilities (exponentially growing long wavelength modes) which can lead to the formation of disoriented chiral condensates (DCCs). We find that instabilities exist for proper times which are less than 3 fm/c. We also show that an experimental signature of domain growth is an increase in the low momentum spectrum of outgoing pions when compared to an expansion in thermal equilibrium. In comparison to particle production during a longitudinal expansion, we find that in a spherical expansion the system reaches the “out” regime much faster and more particles get produced. However the size of the unstable region, which is related to the domain size of DCCs, is not enhanced.

## I. INTRODUCTION

There have been many recent investigations into the formation of disoriented chiral condensates (DCCs) following a relativistic heavy-ion collision [1–3]. The original motivation for studying this problem was the Centauro events [1], rare cosmic ray events in which a deficit of neutral pions was observed [4]. In a recent work [5], the time evolution of the hadronic plasma produced in such a collision was studied by using the  $O(4)$  linear sigma model in a longitudinal expansion. The large- $N$  expansion was used to incorporate non-equilibrium and quantum effects into the problem. After performing numerical simulations to solve the time-dependent equations of motion, instabilities were found to exist for only a short time, and thus no significant amount of pion domains would be formed. In this work, we study the same problem using a spherical expansion, since at late times the expansion becomes spherical. This situation produces the most rapid cooling of the system. We would like to see if the formation of instabilities in this geometry is more pronounced than in a longitudinal expansion.

There are two questions which should be examined. First, we want to know which types of initial conditions lead to the formation of instabilities in the system; and second, if instabilities do form, we want to find out if the size of the unstable region is large enough to see significant domain growth. To answer the first question, we examine the proper-time evolution of the system, starting a short time after the phase transition, where the linear sigma model is appropriate. We look for the effective mass of the pion to go negative during the time evolution. This signifies the onset of growth in long-wavelength modes, which is believed to lead to the formation of DCCs. When we have a case where instabilities form, we then compute the momentum distribution of outgoing pions, and compare to a hydrodynamical model calculation, assuming local thermal equilibrium. We find a noticeable enhancement of low momentum modes as compared to the hydrodynamical model. This provides an experimental signature which can be measured. The implication is that the system is evolving out of thermal equilibrium, which is a necessary condition to have significant growth of low momentum modes.

---

\*e-mail:melissa.lampert@unh.edu

†e-mail:john.dawson@unh.edu

‡e-mail:cooper@pion.lanl.gov

We prepare the initial state of the system in local thermal equilibrium, and study the evolution using scale invariant kinematics ( $v = r/t$ ) to model the cooling of the plasma. Scale invariant kinematics are appropriate for a high energy spherical expansion starting from a point source [6,7], and imply that mean-field expectation values only depend on the proper time  $\tau = \sqrt{t^2 - r^2}$ . We incorporate non-equilibrium and quantum effects through the use of the large- $N$  expansion.

The paper is organized as follows. In Sec. II we describe the linear sigma model to leading order in a  $1/N$  expansion. We then discuss in Sec. III our choice of coordinates and derive equations of motion for the system. We examine issues of renormalization and choice of suitable initial conditions. We also derive an expression for the phase space number density that will be used to calculate momentum distributions. In Sec. IV we discuss the calculation of the energy-momentum tensor, and other thermodynamic relations. In Sec. V we present numerical results of our simulation. In Appendix A we look at properties of the radial functions used in the expansion for the quantum modes. In Appendix B we discuss the transformation of the number density to physically measurable variables.

## II. LINEAR SIGMA MODEL

The Lagrangian density for the linear sigma model in a generalized curvilinear coordinate system is given by:

$$\mathcal{L}[\Phi_i] = \sqrt{-g(x)} \left\{ \frac{1}{2} g_{\mu\nu}(x) [\partial^\mu \Phi_i(x)] [\partial^\nu \Phi_i(x)] - \frac{\lambda}{4} [\Phi_i^2(x) - v^2]^2 \right\}, \quad (2.1)$$

where the mesons are in a  $O(4)$  vector,  $\Phi = (\sigma, \vec{\pi})$ . The factor of  $\sqrt{-g(x)}$ , where  $-g(x) \equiv \det[g_{\mu\nu}(x)]$ , has been introduced to make the Lagrangian a scalar density. The potential here is the ‘‘Mexican hat’’, with degenerate minima at any values of  $\Phi$  such that  $\Phi_i^2 = v^2$ . We will remove this symmetry by introducing a non-zero current term in the  $\sigma$  direction. In this work, we use the convention of an implied sum over a repeated index  $i$ , which runs from 1 to  $N$ . (Here  $N = 4$ .) The counting for the large- $N$  expansion is implemented by introducing a composite field  $\chi = \lambda(\Phi_i^2 - v^2)$ . That is, we add to the Lagrangian a term given by [8]:

$$[\chi - \lambda(\Phi_i^2(x) - v^2)]^2 / 4\lambda.$$

This gives an equivalent Lagrangian,

$$\mathcal{L}[\Phi_i, \chi] = \sqrt{-g(x)} \left\{ \frac{1}{2} g_{\mu\nu}(x) [\partial^\mu \Phi_i] [\partial^\nu \Phi_i] - \frac{1}{2} \chi \Phi_i^2 + \frac{v^2}{2} \chi + \frac{1}{4\lambda} \chi^2 \right\}. \quad (2.2)$$

We can write the action as:

$$S[\Phi_i, \chi; j_i] = \int d^4x \left\{ \mathcal{L}[\Phi_i, \chi] + \sqrt{-g(x)} j_i \Phi_i \right\}. \quad (2.3)$$

We consider the generating functional, given by the path integral,

$$Z[j_i] = \int d[\chi] \int d[\Phi_i] \exp[iS[\Phi_i, \chi; j_i]] \equiv \exp[iW[j_i]].$$

The large- $N$  approximation is equivalent to integrating out the  $\Phi_i$  variables, then performing the remaining  $\chi$  integral using the method of steepest descent. We then Legendre transform to find the effective action,

$$\Gamma[\phi_i, \chi] = W[j_i] - \int d^4x \sqrt{-g(x)} j_i(x) \phi_i(x),$$

where

$$\phi_i(x) = \frac{\delta W}{\delta j_i} \equiv \langle \Phi_i(x) \rangle.$$

We then obtain, to lowest order (in large N)

$$\Gamma[\phi_i, \chi] = \int d^4x \sqrt{-g(x)} \left\{ \frac{1}{2} g_{\mu\nu}(x) [\partial^\mu \phi_i] [\partial^\nu \phi_i] - \frac{1}{2} \chi \phi_i^2 + \frac{v^2}{2} \chi + \frac{1}{4\lambda} \chi^2 + \frac{iN}{2} \ln G_0^{-1}(x, x; \chi) \right\}, \quad (2.4)$$

where

$$(\square + \chi(x))G_0(x, x'; \chi) = i\delta^4(x - x')/\sqrt{-g(x)}.$$

$\Gamma[\phi_i, \chi]$  is the *classical* action plus the trace-log term.

### III. COOLING MECHANISM

#### A. Coordinate System

At late times following a heavy ion collision, the energy flow becomes three-dimensional. If we assume the entire flow is spherical, then the system can be described in terms of the fluid variables:

$$\tau = \sqrt{t^2 - r^2},$$

$$\eta = \tanh^{-1}(r/t) = \frac{1}{2} \ln \left\{ \frac{t+r}{t-r} \right\},$$

where  $t = \tau \cosh \eta$  and  $r = \tau \sinh \eta$ . We restrict the range of these variables to the forward light cone,  $0 \leq \tau < \infty$ , and  $0 \leq \eta < \infty$ . The variables  $\tau$  and  $\eta$  are useful to describe a free spherical expansion of a plasma into the vacuum, with the velocity of the fluid identified as  $v = r/t = \tanh \eta$  [7] when we are at high energies so that the expansion can be thought of as coming from a point source (scaling limit). Minkowski's line element is given by:

$$ds^2 = d\tau^2 - \tau^2 \{ d\eta^2 + \sinh^2 \eta d\theta^2 + \sinh^2 \eta \sin^2 \theta d\phi^2 \},$$

from which we can read off the metric tensor

$$g_{\mu\nu} = \text{diag}(1, -\tau^2, -\tau^2 \sinh^2 \eta, -\tau^2 \sinh^2 \eta \sin^2 \theta),$$

$$\sqrt{-g} = \tau^3 \sinh^2 \eta \sin \theta.$$

This can be compared to the Robertson-Walker metric for spherical geometry, given by the line element:

$$ds^2 = d\tau^2 - a^2(\tau) \{ d\eta^2 + \sinh^2 \eta d\theta^2 + \sinh^2 \eta \sin^2 \theta d\phi^2 \}.$$

Thus the case we consider here corresponds to a cosmological model with a fixed uniform expansion proportional to the proper time  $\tau$ , and zero curvature.

#### B. Equations of motion

We can derive the equations of motion from the effective action, (2.4). Varying the action with respect to  $\phi_i$  and  $\chi$  gives:

$$(\square + \chi(x))\phi_i(x) = j_i(x) \equiv H\delta_{i0}$$

$$(\square + \chi(x))G_0(x, x') = i\delta^4(x - x')/\sqrt{-g(x)}, \quad (3.1)$$

and the gap equation

$$\chi(x) = \lambda \{ -v^2 + \phi_i^2(x) + NG_0(x, x) \} . \quad (3.2)$$

In order to give the pions mass, it is only necessary to have a current in the zero ( $\sigma$ ) direction, so that  $j_0(x) \equiv H = \text{constant}$ .

We determine the parameters in the model by considering the vacuum sector. Spatial homogeneity then gives:

$$\begin{aligned} \chi_0 \sigma_0 &= H , \\ \chi_0 &= -\lambda v^2 + \lambda \sigma_0^2 + \lambda N \int \frac{k^2 dk}{2\pi^2} \frac{1}{2\sqrt{k^2 + \chi_0}} . \end{aligned}$$

The PCAC (partial conservation of axial vector current) condition gives:

$$\partial_\mu A_i^\mu(x) = H \pi_i(x) ,$$

where the axial vector current is given by

$$A_i^\mu(x) = [\pi_i(x) \partial^\mu \sigma(x) - \sigma(x) \partial^\mu \pi_i(x)] ,$$

which leads to

$$H = f_\pi m^2 .$$

Since we have defined the vacuum by  $\chi_0 \sigma_0 = m^2 \sigma_0 = H$ , we then find that  $\sigma_0 = f_\pi$ . The coupling constant  $\lambda$  is determined by the low-energy  $\pi - \pi$  scattering data, as described in [5].

We now specialize to the case when  $\phi_i$  and  $\chi$  are functions of  $\tau$  only. We can see that (3.1) is also the equation for a free scalar quantum field with a time-dependent mass  $\chi(\tau)$ , which is self-consistently determined by (3.2). Therefore we can introduce a quantum field  $\Phi_i = \phi_i + \hat{\phi}_i$ . The equations for  $\Phi_i$  are:

$$\begin{aligned} \left\{ \frac{1}{\tau^3} \frac{\partial}{\partial \tau} \left( \tau^3 \frac{\partial}{\partial \tau} \right) + \chi(\tau) \right\} \phi_i(\tau) &= H \delta_{i0} \\ (\square + \chi(\tau)) \hat{\phi}_i(x) &= 0 , \end{aligned} \quad (3.3)$$

where the 4-vector  $x = (\tau, \eta, \theta, \phi)$ . Then for  $G_0$  we find:

$$G_0(x, x') \equiv \langle T_c \{ \hat{\phi}(x, \tau), \hat{\phi}(x', \tau') \} \rangle ,$$

where  $T_c$  corresponds to a  $\tau$ -ordered product [9], following the closed-time-path formalism of Schwinger. When  $\langle \pi^i \rangle = 0$ , this is the true Green's function.

Following Parker and Fulling [10], we expand  $\hat{\phi}_i$  into a complete set of states,

$$\begin{aligned} \hat{\phi}_i(\tau, \eta, \theta, \phi) &= \int_0^\infty ds \sum_{lm} [\hat{a}_{i,slm} \psi_s(\tau) \mathcal{Y}_{slm}(\eta, \theta, \phi) \\ &\quad + \text{h.c.}] \end{aligned} \quad (3.4)$$

with

$$\mathcal{Y}_{slm}(\eta, \theta, \phi) = \pi_{sl}(\eta) Y_{lm}(\theta, \phi) , \quad (3.5)$$

and where  $\psi$ ,  $\pi$ , and  $Y$  satisfy:

$$\begin{aligned} \left[ \frac{1}{\tau^3} \frac{\partial}{\partial \tau} \left( \tau^3 \frac{\partial}{\partial \tau} \right) + \frac{s^2 + 1}{\tau^2} + \chi(\tau) \right] \psi_s &= 0 , \\ \left[ \frac{1}{\sinh^2 \eta} \frac{\partial}{\partial \eta} \left( \sinh^2 \eta \frac{\partial}{\partial \eta} \right) + s^2 + 1 - \frac{l(l+1)}{\sinh^2 \eta} \right] \pi_{sl} &= 0 , \end{aligned}$$

$$\left[ \frac{1}{\sin \theta} \frac{\partial}{\partial \theta} \left( \sin \theta \frac{\partial}{\partial \theta} \right) + \frac{1}{\sin^2 \theta} \left( \frac{\partial^2}{\partial \phi^2} \right) + l(l+1) \right] Y_{lm} = 0.$$

Here,  $Y_{lm}(\theta, \phi)$  are the usual spherical harmonics, and  $\pi_{sl}(\eta)$  are a complete set of functions, discussed in Appendix A.

In order to satisfy the canonical commutation relations, we require  $\psi_s(\tau)$  to satisfy the Wronskian condition:

$$\psi_s^*(\tau) \dot{\psi}_s(\tau) - \psi_s(\tau) \dot{\psi}_s^*(\tau) = -i/\tau^3,$$

where the ‘‘dot’’ means differentiation with respect to  $\tau$ . Therefore we find

$$[\hat{\phi}_{i,slm}(\tau), \hat{\phi}_{j,s'l'm'}^\dagger(\tau)] = i\delta_{ij} \delta(s' - s) \delta_{ll'} \delta_{mm'} / \tau^3,$$

and

$$[\hat{a}_{i,slm}, \hat{a}_{j,s'l'm'}^\dagger] = \delta_{ij} \delta(s' - s) \delta_{ll'} \delta_{mm'}.$$

We are now in a position to calculate  $\langle \hat{\phi}_i^2 \rangle$ . We shall choose the (Heisenberg) state vector such that the bilinear forms of creation and destruction operators are diagonal:

$$\begin{aligned} \langle \hat{a}_{j,s'l'm'}^\dagger \hat{a}_{i,slm} \rangle &= n_s \delta_{ij} \delta(s' - s) \delta_{ll'} \delta_{mm'}, \\ \langle \hat{a}_{j,s'l'm'} \hat{a}_{i,slm}^\dagger \rangle &= (n_s + 1) \delta_{ij} \delta(s' - s) \delta_{ll'} \delta_{mm'}, \\ \langle \hat{a}_{j,s'l'm'} \hat{a}_{i,slm} \rangle &= p_s \delta_{ij} \delta(s' - s) \delta_{ll'} \delta_{mm'}, \\ \langle \hat{a}_{j,s'l'm'}^\dagger \hat{a}_{i,slm}^\dagger \rangle &= p_s^* \delta_{ij} \delta(s' - s) \delta_{ll'} \delta_{mm'}. \end{aligned}$$

Here  $n_s$  and  $p_s$  are the particle and pair densities. They will be taken to be a function of  $s$  only. In addition, we will take  $n_s$  to be a thermal distribution in the comoving frame,

$$n_s = \frac{1}{e^{\omega_s(\tau_0)/k_B T} - 1},$$

with  $\omega_s = \sqrt{s^2/\tau_0^2 + \chi(\tau_0)}$ . We can choose  $p_s = 0$  for all our simulations, since one has the freedom to make a Bogoliubov transformation at  $\tau_0$  so that this is true. Using the results in Appendix A, we then find

$$\begin{aligned} \langle \hat{\phi}_i^2 \rangle &= \int_0^\infty ds (2n_s + 1) |\psi_s(\tau)|^2 \sum_{lm} |\mathcal{Y}_{slm}(\eta, \theta, \phi)|^2 \\ &= \int_0^\infty \frac{s^2 ds}{2\pi^2} (2n_s + 1) |\psi_s(\tau)|^2. \end{aligned}$$

Therefore (3.2) becomes:

$$\chi(\tau) = -\lambda v^2 + \lambda \phi_i^2(\tau) + \lambda N \int_0^\infty \frac{s^2 ds}{2\pi^2} (2n_s + 1) |\psi_s(\tau)|^2, \quad (3.6)$$

and is a function of  $\tau$  only. This completes the derivation of the equations of motion.

### C. Initial Conditions and Renormalization

The variable  $\tau$  does not allow for a good WKB expansion due to the singularity at  $\tau = 0$ . The transformation  $u = \ln(m\tau)$ , where  $m$  is any mass scale (we choose  $m = m_\pi$ ), maps the singularity to  $u = -\infty$ , and allows one to perform a WKB expansion in the usual manner.

Changing variables to  $u$  and rescaling the fields using the substitutions

$$\begin{aligned} \psi_s(u) &= g_s(u) e^{-u} m^{3/2} \\ \phi_i(u) &= \rho_i(u) e^{-u} m^{3/2}, \end{aligned}$$

we get:

$$\begin{aligned} \left[ \frac{d^2}{du^2} + s^2 + \chi(u)e^{2u}/m^2 \right] g_s(u) &= 0 \\ \left[ \frac{d^2}{du^2} + \chi(u)e^{2u}/m^2 - 1 \right] \rho_i(u) &= H\delta_{i0}e^{3u}/m^{7/2} \end{aligned} \quad (3.7)$$

with

$$\begin{aligned} \chi(u) &= -\lambda v^2 + \lambda \sum_i m^3 e^{-2u} \rho_i^2(u) \\ &+ \lambda N \int_0^{s_m} \frac{s^2 ds}{2\pi^2} (2n_s + 1) m^3 e^{-2u} |g_s(u)|^2, \end{aligned} \quad (3.8)$$

with  $s_m = \Lambda e^u/m$ . Then  $g_s(u)$  obeys the Wronskian

$$g_s^*(u) \frac{dg_s(u)}{du} - \frac{dg_s^*(u)}{du} g_s(u) = -i/m.$$

From (3.7), we notice that when  $\chi(u) < 0$ , modes satisfying  $s^2/\tau^2 < \chi$  grow exponentially in  $\tau$ . However, from (3.8), we see that these growing modes will quickly cause  $\chi$  to become positive when  $\lambda$  is large, as is the case here.

We can now use a WKB ansatz for  $g_s(u)$ :

$$g_s(u) = \frac{1}{\sqrt{2mW_s(u)}} \exp \left[ -i \int_{u_0}^u W_s(u') du' \right],$$

where  $W_s(u)$  satisfies:

$$\frac{1}{2} \frac{W_s''}{W_s} - \frac{3}{4} \left( \frac{W_s'}{W_s} \right)^2 + W_s^2 = \omega_s^2(u), \quad (3.9)$$

and  $\omega_s(u) = \sqrt{s^2 + \chi(u)e^{2u}/m^2}$ . We will then take the initial conditions

$$\begin{aligned} W_s(u_0) &= \omega_s(u_0) \\ W_s'(u_0) &= \omega_s'(u_0), \end{aligned}$$

which correspond to the adiabatic vacuum. This allows us to introduce an interpolating number density which interpolates between  $n_s(u)$  and the true ‘‘out’’ density,  $n_{\text{out}}$ .

By a WKB analysis, one can show [11] that  $G_0(x, x)$  has quadratic and logarithmic divergences. The quadratic divergence can be removed by mass renormalization. In the vacuum sector, the mass of the pion is given by (3.8), with  $\chi_{\text{vac}} \equiv m_\pi^2 = m^2$ :

$$m^2 = -\lambda v^2 + \lambda f_\pi^2 + \lambda N \int_0^\Lambda \frac{k^2 dk}{2\pi^2} \frac{1}{2\sqrt{k^2 + m^2}}, \quad (3.10)$$

with cutoff  $\Lambda$ . We note that if we change variables in the integral to  $s = k\tau = ke^u/m$ , (3.10) becomes:

$$\begin{aligned} m^2 &= -\lambda v^2 + \lambda f_\pi^2 \\ &+ \lambda N m^2 e^{-2u} \int_0^{s_m} \frac{s^2 ds}{2\pi^2} \frac{1}{2\sqrt{s^2 + e^{2u}}}. \end{aligned} \quad (3.11)$$

Subtracting this equation from (3.8), we obtain a logarithmically divergent expression for  $\chi$ :

$$\begin{aligned} \chi(u) &= m^2 + \lambda \sum_i (m^3 e^{-2u} \rho_i^2(u) - f_\pi^2) \\ &+ \lambda N \int_0^{s_m} \frac{s^2 ds}{2\pi^2} (2n_s + 1) m^3 e^{-2u} |g_s(u)|^2 \\ &- \lambda N \int_0^{s_m} \frac{s^2 ds}{2\pi^2} m^2 e^{-2u} \frac{1}{2\sqrt{s^2 + e^{2u}}}. \end{aligned} \quad (3.12)$$

Note that the last integral is *independent* of  $u$ .

The coupling constant is renormalized by taking

$$\begin{aligned}\frac{1}{\lambda} &= \frac{1}{\lambda_r} - \frac{N}{8\pi^2} \int_0^\Lambda \frac{k^2 dk}{(k^2 + m^2)^{3/2}} \\ &= \frac{1}{\lambda_r} - \frac{N}{8\pi^2} \int_0^{s_m} \frac{s^2 ds}{(s^2 + e^{2u})^{3/2}}.\end{aligned}\quad (3.13)$$

One can explicitly show by using (3.13) in (3.12) that  $\chi(u)$  is now completely finite.

We will also need the value of  $\dot{\chi}(u)$  for the initial conditions:

$$\begin{aligned}\dot{\chi}(u) &\left[ 1 + \lambda N \int_0^{s_m} \frac{s^2 ds}{2\pi^2} (2n_s + 1) \frac{1}{4\omega_s^3(u)} \right] \\ &= 2\lambda e^{-2u} m^3 [\rho_i(u)\rho_i'(u) - \rho_i^2(u)] \\ &+ \frac{\lambda N \Lambda^3}{4\pi^2} \frac{(2n_{s_m} + 1)}{\sqrt{\Lambda^2 + \chi(u)}} \\ &- \lambda N \int_0^{s_m} \frac{s^2 ds}{2\pi^2} (2n_s + 1) m^2 e^{-2u} \\ &\quad \times \left[ \frac{\chi(u)e^{2u}}{2m^2\omega_s^3(u)} + \frac{1}{\omega_s(u)} \right].\end{aligned}\quad (3.14)$$

#### D. Phase Space Interpolating Number Density

In the expansion (3.4), we can also use a time-dependent set of creation and annihilation operators, with first order adiabatic mode functions,

$$\begin{aligned}\hat{\phi}_i(u, \eta, \theta, \phi) &= \int_0^\infty ds \sum_{lm} [\hat{a}_{i,slm}(u) \psi_s^0(u) \mathcal{Y}_{slm}(\eta, \theta, \phi) \\ &\quad + \text{h.c.}]\end{aligned}\quad (3.15)$$

where

$$\psi_s^0(u) = g_s^0(u) e^{-u} m^{3/2},$$

and

$$g_s^0(u) = \frac{1}{\sqrt{2m\omega_s(u)}} \exp \left[ -i \int_{u_0}^u \omega_s(u') du' \right].$$

We can define the first order adiabatic number density as:

$$n_s(u) = \langle \hat{a}_s^\dagger(u) \hat{a}_s(u) \rangle, \quad (3.16)$$

where, for simplicity, we have suppressed the angular indices on  $\hat{a}_s$  and  $\hat{a}_s^\dagger$ .

One can show [12] that  $n_s(u)$  is an adiabatic invariant, and would be the true number density in a slowly varying expansion. We then choose

$$\begin{aligned}\hat{a}_s &= \hat{a}_s(u_0) \\ g_s(u_0) &= g_s^0(u_0)\end{aligned}$$

so that the initial  $\hat{a}$  and  $\hat{a}^\dagger$  are the adiabatic ones. When  $\chi(u) \rightarrow m^2$  then  $n_s(u) \rightarrow n_{\text{out}}$ , which is the true out-state phase space number density.

The time-dependent creation and annihilation operators satisfy

$$\frac{d\hat{a}_s}{du}g_s^0 + \frac{d\hat{a}_s^\dagger}{du}g^{0*} = 0. \quad (3.17)$$

The time-dependent operators can be connected to the time-independent operators via a Bogoliubov transformation:

$$\hat{a}_s(u) = \alpha(s, u)\hat{a}_s + \beta(s, u)\hat{a}_{-s}^\dagger, \quad (3.18)$$

where  $\alpha$  and  $\beta$  are determined by:

$$\begin{aligned} \alpha(s, u) &= i \left( g_s^{0*} \frac{dg_s}{du} - \frac{dg_s^{0*}}{du} g_s \right) \\ \beta(s, u) &= i \left( g_s^0 \frac{dg_s}{du} - \frac{dg_s^0}{du} g_s \right). \end{aligned} \quad (3.19)$$

We then find

$$n_s(u) = n_s(u_0) + |\beta(s, u)|^2(1 + 2n_s(u_0)). \quad (3.20)$$

Notice that at  $u = u_0$ ,  $\beta(s, u_0) = 0$ , so  $n_s(u) = n_s(u_0) \equiv n_s$ . Since  $n_s(u_0)$  is the initial phase space number density, and at late times, becomes the out-state number density, it is an interpolating number density.

#### IV. ENERGY-MOMENTUM TENSOR

The energy-momentum tensor  $T^{\mu\nu}$  is defined by:

$$\delta S = -\frac{1}{2} \int d^4x \sqrt{-g} T^{\mu\nu}(x) \delta g_{\mu\nu}(x), \quad (4.1)$$

with the action given by (2.3). Performing the variations, we find the ‘‘improved’’ energy-momentum tensor [13]

$$\begin{aligned} T_{\mu\nu}(x) &= (\partial_\mu \Phi_i)(\partial_\nu \Phi_i) - g_{\mu\nu} \mathcal{L} \\ &\quad + \frac{1}{6} [g_{\mu\nu} g^{\alpha\beta} \Phi_{i;\alpha;\beta}^2 - \Phi_{i;\mu;\nu}^2], \end{aligned} \quad (4.2)$$

where the Lagrangian density is given by (2.2). We follow the standard practice [7] and define the energy density and pressures by

$$T_{\mu\nu} = \text{diag}(\epsilon, p_\eta \tau^2, p_\theta \tau^2 \sinh^2 \eta, p_\phi \tau^2 \sinh^2 \eta \sin^2 \theta).$$

Next, we take expectation values of the energy-momentum tensor. One can easily show all the pressures are equal,  $p = p_\eta = p_\theta = p_\phi$ , and that  $T_{\mu\nu}$  is diagonal.

The energy-momentum tensor obeys a conservation law:

$$T_{;\mu}^{\mu\nu} = \frac{1}{\sqrt{-g}} \frac{\partial}{\partial x^\mu} (\sqrt{-g} T^{\mu\nu}) + \Gamma_{\mu\lambda}^\nu T^{\mu\lambda} = 0. \quad (4.3)$$

One can easily verify that the energy conservation equation, the  $\nu = 0$  component of (4.3) takes the form:

$$\frac{\partial \epsilon}{\partial \tau} + \frac{3}{\tau}(\epsilon + p) = 0. \quad (4.4)$$

In thermal equilibrium, this would become the entropy conservation equation. Then we have  $d\epsilon = T ds$  and  $\epsilon + p = Ts$ . In an ultra-relativistic fluid expansion, with  $c_0^2 = \frac{1}{3}$ ,  $p = \frac{1}{3}\epsilon$  and  $\epsilon\tau^4 = \text{constant}$ .

In our simulations we have verified that the local energy conservation (4.3) is valid.

## V. NUMERICAL RESULTS

To choose the initial conditions, we start the system at a temperature above the phase transition in thermal equilibrium, with all particle masses positive. The equations are solved self-consistently at the starting time to obtain the values of the  $\chi$ ,  $\langle\sigma\rangle$  and  $\langle\vec{\pi}\rangle$  fields. We fixed the value of  $\chi$  at the initial time as the solution of the gap equation in the initial thermal state. We also required that the initial expectation values of the  $\sigma$  and  $\vec{\pi}$  fields satisfy

$$\pi^2(\tau_0) + \sigma^2(\tau_0) = \sigma_T^2,$$

where  $\sigma_T$  is the equilibrium value of  $\Phi$  at the initial temperature  $T$ . We choose  $T = 200$  MeV, which gives  $\sigma_T = 0.3$  fm<sup>-1</sup>. We compute the time evolution of these fields, starting at a proper time  $\tau_0 = 1$  fm. The value of  $f_\pi$  used in all the simulations is 92.5 MeV, and  $\lambda_R$  is 7.3 (see [5]). Below we show results for several sets of initial conditions. Once the initial values are chosen, we have the freedom to vary the first derivative of the  $\Phi$  field. The results with  $\dot{\pi} \neq 0$  were similar to those with  $\dot{\sigma} \neq 0$ , so we only show results for the latter case. We find there is a wide range of values which will allow the system to become unstable,  $0.15 < |\dot{\sigma}| < 4.95$ . This can be compared with the longitudinal expansion [5], where the regime of instability was much smaller,  $0.25 < |\dot{\sigma}| < 1.3$ . This is because the spherical expansion leads to a much larger negative gradient for  $\chi$  than the longitudinal case.

Figures 1 and 2 show the results of the numerical simulation for the proper time evolution of the system. We display the auxiliary field  $\chi$  in units of fm<sup>-2</sup>, the classical fields  $\Phi_i$  in units of fm<sup>-1</sup>, and the proper time in units of fm. At proper times greater than  $\approx 10$  fm, the auxiliary field reaches its vacuum value of  $m_\pi^2$ , the  $\sigma$  field approaches its vacuum value of  $f_\pi$ , and the  $\pi$  field its value of zero. This is in distinction to the longitudinal expansion, where even at  $\tau = 30$  fm, one had not yet reached the “out” regime.

For all of our initial conditions, the size of the unstable region ( $\chi < 0$ ) is at most 2-3 fm. Thus we find that the spherical expansion does not produce larger domains than the longitudinal case. We also see that when we start the initial expectation value of  $\Phi_i$  in the  $\pi_1$  direction that the system becomes slightly more unstable. We notice that if the derivative of the field is positive or zero that this is insufficient to generate instabilities.

In Fig. 3, we show the effect of the initial temperature on the evolution of the auxiliary field. We see that varying the initial temperature has little effect. In Fig. 4, we show the evolution of the  $\chi$  field for different values of the cutoff  $\Lambda$ . We can see that  $\chi$  is independent of  $\Lambda$ , which shows that the renormalization has been carried out correctly. In our simulations we use the value  $\Lambda = 800$  MeV, since  $\Lambda = 1$  GeV is too close to the Landau pole (see [5]). When one chooses a cutoff too close to the Landau pole the late time behavior becomes unstable.

Figures 5 and 6 show the number density calculated from (3.20), for several different proper times. Figure 5 is a case where instabilities have arisen in the system, and there is a large amount of particle production during the time that  $\chi$  has gone negative. Figure 6 is a case with no instabilities, and there is very little particle production as a function of proper time.

Figures 7 and 8 show the same distributions transformed to the physical momentum  $p$ , as discussed in Appendix B. The momentum  $p$  is plotted in units of  $m_\pi$ . We compare these distributions to a hydrodynamical model calculation [see (B3)], where we have assumed that when the system reaches the “out” regime, the final distribution is a combination of a thermal distribution in the comoving frame at  $T_c = m_\pi$  boosted to the center of mass frame using the boost variable  $\eta(r, t)$  (see [7]). For comparison purposes, we have renormalized the thermal distributions to give the same center of mass energy ( $E = 100$  GeV) as the corresponding non-thermal distributions. We see that as a result of the non-equilibrium evolution, there is an enhancement at low momentum independent of whether or not there are instabilities; however, the effect of instabilities is to greatly magnify this low momentum enhancement.

## VI. CONCLUSIONS

In this paper we have performed numerical simulations to examine the chiral phase transition during a uniform spherical expansion of the hadronic plasma. We used the linear  $\sigma$  model to leading order in a large- $N$  expansion and studied a wide range of initial conditions starting above the critical temperature for the phase transition. We found initial conditions which drove the system to instabilities that lead to the formation of disoriented chiral condensates. Due to the necessity of a rather large renormalized coupling constant, the formation of instabilities lasted only a short time because of the large exponentially growing quantum corrections in (3.8), and no significant amount of domain formation was observed. However, we find that the phase space number density for our non-equilibrium evolution is significantly different from one which would result from an evolution in thermal equilibrium. The experimental signature for domain formation is an increase in the pion particle production rate at low momentum. Our calculations were done in a mean-field approximation, where all the mode coupling is due to the presence of this mean field. In next order in large- $N$ , scattering in the background mean field occurs, and the possibility for re-equilibration exists.

These effects will be incorporated in a future calculation. In comparison to particle production during a longitudinal expansion, we find that in a spherical expansion the system reaches the “out” regime much faster and more particles get produced. However the size of the unstable region, which is related to the size of the domain of DCCs, is not enhanced.

### ACKNOWLEDGEMENTS

The authors would like to thank Emil Mottola, Yuval Kluger and Salman Habib for useful discussions. UNH gratefully acknowledges support by the U.S. Department of Energy (DE-FG02-88ER40410). One of us (FC) would like to thank the University of New Hampshire for its hospitality.

### APPENDIX A: PROPERTIES OF THE $\pi_{SL}$ FUNCTIONS

In this appendix, we discuss properties of the functions  $\pi_{sl}(\eta)$ , which are *real* solutions of the equation,

$$\frac{1}{\sinh^2 \eta} \frac{\partial}{\partial \eta} \left( \sinh^2 \eta \frac{\partial \pi_{sl}}{\partial \eta} \right) + \left\{ s^2 + 1 - \frac{l(l+1)}{\sinh^2 \eta} \right\} \pi_{sl} = 0,$$

or,

$$\frac{\partial^2 \pi_{sl}}{\partial \eta^2} + \frac{2}{\tanh \eta} \frac{\partial \pi_{sl}}{\partial \eta} + \left\{ s^2 + 1 - \frac{l(l+1)}{\sinh^2 \eta} \right\} \pi_{sl} = 0,$$

for  $\eta$  in the range:  $0 \leq \eta \leq \infty$ . With the substitution,

$$\pi_{sl}(\eta) = u_{sl}(\eta) / \sinh \eta,$$

we find that  $u_{sl}(\eta)$  satisfies:

$$u_{sl}'' + \left[ s^2 - \frac{l(l+1)}{\sinh^2 \eta} \right] u_{sl} = 0.$$

The general solution is given by [14]:

$$\pi_{sl}(\eta) = \frac{\sinh^l \eta}{M_{sl}} \left( \frac{d}{d \cosh \eta} \right)^{(1+l)} \cos(s\eta),$$

where the normalization  $M_{sl}$  is given by

$$M_{sl} = \sqrt{(\pi/2)s^2(s^2+1^2)\dots(s^2+l^2)}.$$

The completeness relation is given by:

$$\int_0^\infty ds \pi_{sl}(\eta) \pi_{sl}(\eta') = \delta(\eta - \eta') / [\sinh \eta \sinh \eta'].$$

For the functions  $\mathcal{Y}_{slm}$  defined in (3.5), the addition formula is [10]:

$$\begin{aligned} & \sum_{lm} \mathcal{Y}_{slm}^*(\eta_1, \theta_1, \phi_1) \mathcal{Y}_{slm}(\eta_2, \theta_2, \phi_2) \\ &= \frac{s}{2\pi^2} \frac{\sin(s\eta)}{\sinh \eta} = \frac{s^2}{2\pi^2} \left\{ 1 - \frac{s^2+1}{6} \eta^2 + \dots \right\}, \end{aligned}$$

where  $\eta$  is defined by:

$$\begin{aligned} \cosh \eta &= \cosh \eta_1 \cosh \eta_2 - \sinh \eta_1 \sinh \eta_2 \cos \theta \\ \cos \theta &= \cos \theta_1 \cos \theta_2 + \sin \theta_1 \sin \theta_2 \cos(\phi_1 - \phi_2). \end{aligned}$$

Therefore, taking the limit,  $(\eta_1, \theta_1, \phi_1) \rightarrow (\eta_2, \theta_2, \phi_2)$ , or  $\eta \rightarrow 0$ , we find

$$\sum_{lm} |\mathcal{Y}_{slm}(\eta, \theta, \phi)|^2 = \frac{s^2}{2\pi^2}.$$

By differentiating both sides of the addition formula, we can show that

$$\begin{aligned} \sum_{lm} \left| \frac{\partial \mathcal{Y}_{slm}(\eta, \theta, \phi)}{\partial \eta} \right|^2 &= \frac{s^2}{2\pi^2} \left( \frac{s^2 + 1}{3} \right), \\ \sum_{lm} \left| \frac{\partial \mathcal{Y}_{slm}(\eta, \theta, \phi)}{\partial \theta} \right|^2 &= \frac{s^2}{2\pi^2} \left( \frac{s^2 + 1}{3} \right) \sinh^2 \eta, \\ \sum_{lm} \left| \frac{\partial \mathcal{Y}_{slm}(\eta, \theta, \phi)}{\partial \phi} \right|^2 &= \frac{s^2}{2\pi^2} \left( \frac{s^2 + 1}{3} \right) \sinh^2 \eta \sin^2 \theta. \end{aligned}$$

## APPENDIX B: TRANSFORMATION TO PHYSICAL VARIABLES

In terms of the initial distribution of particles  $n_s(\tau_0)$  and  $\beta$  we have:

$$n_s(u) = n_s(u_0) + |\beta(s, u)|^2 (1 + 2n_s(u_0)),$$

where  $n_s(u)$  is the adiabatic invariant interpolating phase space number density which becomes the actual particle phase space number density in the comoving frame when interactions have ceased. We now need to relate this quantity to the physical spectra of particles measured in the lab. At late  $\tau \geq \tau_f \approx 10$  fm our system relaxes to the vacuum and  $\chi$  becomes the square of the physical pion mass  $m^2$ . The comoving center of mass energy of outgoing particles can then be identified with

$$\omega_s(\tau_f) = \sqrt{\frac{s^2}{\tau_f^2} + m^2}.$$

The actual distribution of momenta in the lab frame is a combination of the collective (“fluid”) motion described by the boost  $\eta$  from the comoving frame to center of mass frame and the comoving particle distribution. Here, the space-like hypersurface on which one is counting particles is at fixed proper time  $\tau_f$ . This distribution is given by the Cooper-Frye formula [15] which is:

$$E \frac{dN}{d^3p} = E \frac{dN}{4\pi p^2 dp} = \int f(x, p) p^\mu d\sigma_\mu. \quad (\text{B1})$$

We identify the relativistic phase space distribution function  $f(x, p)$  with  $n_s(u_f)$ . The dependence of  $s$  on the space time variable  $x$  and the outgoing momentum  $p$  is found from the relationship

$$p^\mu u_\mu = \omega_s(\tau_f) = \sqrt{\frac{s^2}{\tau_f^2} + m^2}.$$

We choose the measured momentum  $p$  to be in the  $z$  direction  $\hat{e}_3$  of our spherical coordinate system. We have that

$$\begin{aligned} u^\mu &= (\cosh \eta, \sinh \eta \hat{e}_r) \\ p^\mu &= (E, p \hat{e}_3), \end{aligned}$$

so that

$$p^\mu u_\mu = E \cosh \eta - p \cos \theta \sinh \eta.$$

The surface on which one is counting particles is the time-like surface  $\tau = \tau_f$  with

$$d\sigma_\mu = \left(1, -\frac{\partial t_f}{\partial r} \hat{e}_r\right) d^3r.$$

Changing variables from  $r$  to  $\eta$  at fixed  $\tau$  we then obtain

$$\begin{aligned} E \frac{dN}{4\pi p^2 dp} &= n(p, \tau) \\ &= \int f(x, p) d\eta d\cos\theta \tau_f^3 \sinh^2 \eta p^\mu u_\mu, \end{aligned} \quad (\text{B2})$$

where

$$p^\mu u_\mu = E \cosh \eta - p \cos \theta \sinh \eta$$

and we have used the isotropy assumption and chosen  $p$  as the  $z$  axis. Here  $E = \sqrt{p^2 + m^2}$ .

The calculation that (B2) needs to be compared with is a hydrodynamical model calculation for a local thermal equilibrium flow. In a hydrodynamical model of heavy ion collisions [6,7], the final spectrum of pions is given by a combination of the fluid flow and a local thermal equilibrium distribution in the comoving frame. One calculates this spectrum at the critical temperature  $T_c(x, t)$  when the energy density goes below

$$\epsilon_c = \frac{1}{(\hbar/mc)^3}.$$

This defines the breakup surface  $\tau_c$ , after which the particles no longer interact so that this distribution is frozen at that temperature. For an ultrarelativistic gas of pions, this occurs when  $T_c = m$ . The covariant form for the spectra of particles is again given by the Cooper-Frye formula [15]:

$$E \frac{dN}{4\pi p^2 dp} = \int f(x, p) d\eta d\cos\theta \tau_c^3 \sinh^2 \eta p^\mu u_\mu \quad (\text{B3})$$

but now  $f(x, p)$  is the single particle relativistic phase space distribution function for pions in local thermal equilibrium at a comoving temperature  $T_c(\tau_c)$ :

$$f(x, p) = \{\exp[p^\mu u_\mu / T_c] - 1\}^{-1}.$$

We have identified the left hand side of (B3) as  $n_{th}(p, \tau)$ .

- [1] A. Anselm, Phys. Lett. B **217**, 169 (1989); A. Anselm and M. Ryskin, *ibid* **226**, 482 (1991)
- [2] J.D. Bjorken, Int. J. Mod. Phys. A **7**, 4189 (1992); Acta Phys. Pol. B **23**, 561 (1992).
- [3] K. Rajagopal and F. Wilczek, Nucl. Phys. **B399**, 395 (1993);  
S. Gavin, A. Gocksch and R.D. Pisarski, Phys. Rev. Lett. **72**, 2143 (1994);  
S. Gavin and B. Müller, Phys. Lett. B **329**, 486 (1994);  
S. Gavin, hep-ph/9407368;  
D. Boyanovsky, H.J. de Vega, and R. Holman, Phys. Rev. D **51**, 734 (1995);  
J.-P. Blaizot and A. Krzywicki, Phys. Rev. D **46**, 246 (1992); Phys. Rev. D **50**, 442 (1994).
- [4] C.M.G. Lattes, Y. Fujimoto, and S. Hasegawa, Phys. Rep. **65**, 151 (1980).
- [5] F. Cooper, Y. Kluger, E. Mottola, and J. P. Paz, Phys. Rev. D **51**, 2377 (1995).
- [6] J. D. Bjorken, Phys. Rev. D **27**, 140 (1983).
- [7] Fred Cooper, Graham Frye, and Edmond Schonberg, Phys. Rev. D **11**, 192 (1975).
- [8] H. E. Stanley, Phys. Rev. **176**, 718 (1968);  
K. Wilson, Phys. Rev. D **7**, 2911 (1973);  
S. Coleman, R. Jackiw, and H. D. Politzer, Phys. Rev. D **10**, 2491 (1974).
- [9] J. Schwinger, J. Math. Phys. **2**, 407 (1961);  
P. M. Bakshi and K. T. Mahanthappa, J. Math. Phys. **4**, 1 (1963); **4**, 12 (1963);  
L. V. Keldysh, Zh. Eksp. Teo. Fiz. **47**, 1515 (1964) [Sov. Phys. JETP **20**, 1018 (1965)];  
G. Zhou, Z. Su, B. Hao and L. Yu, Phys. Rep. **118**, 1 (1985);  
F. Cooper, S. Habib, Y. Kluger, E. Mottola, J.P. Paz and Paul Anderson, Phys. Rev. D **50**, 2848 (1994).

- [10] L. Parker and S. A. Fulling, Phys. Rev. D **9**, 341 (1974).  
[11] F. Cooper and E. Mottola, Phys. Rev. D **36**, 3114 (1987).  
[12] Salman Habib, Yuval Kluger, Emil Mottola, and Juan Pablo Paz, Los Alamos Preprint (LA-UR-95-3393/LBL-37786), 1995.  
[13] C. G. Callan, S. Coleman, and R. Jackiw, Ann. Phys. (NY) **59**, 42 (1970).  
[14] N.D. Birrell and P.C.W. Davies, *Quantum Fields in Curved Space*, (Cambridge University Press, 1982), p. 122.  
[15] F. Cooper and G. Frye, Phys. Rev. D **10**, 186 (1974). See also “Fireball Spectra” by Ekkard Schnedermann, Josef Sollfrank, and Ulrich Heinz in *Particle Production in Highly Excited Matter*, pp. 175-206, edited by H.H. Gutbrod (Plenum, New York, 1993).

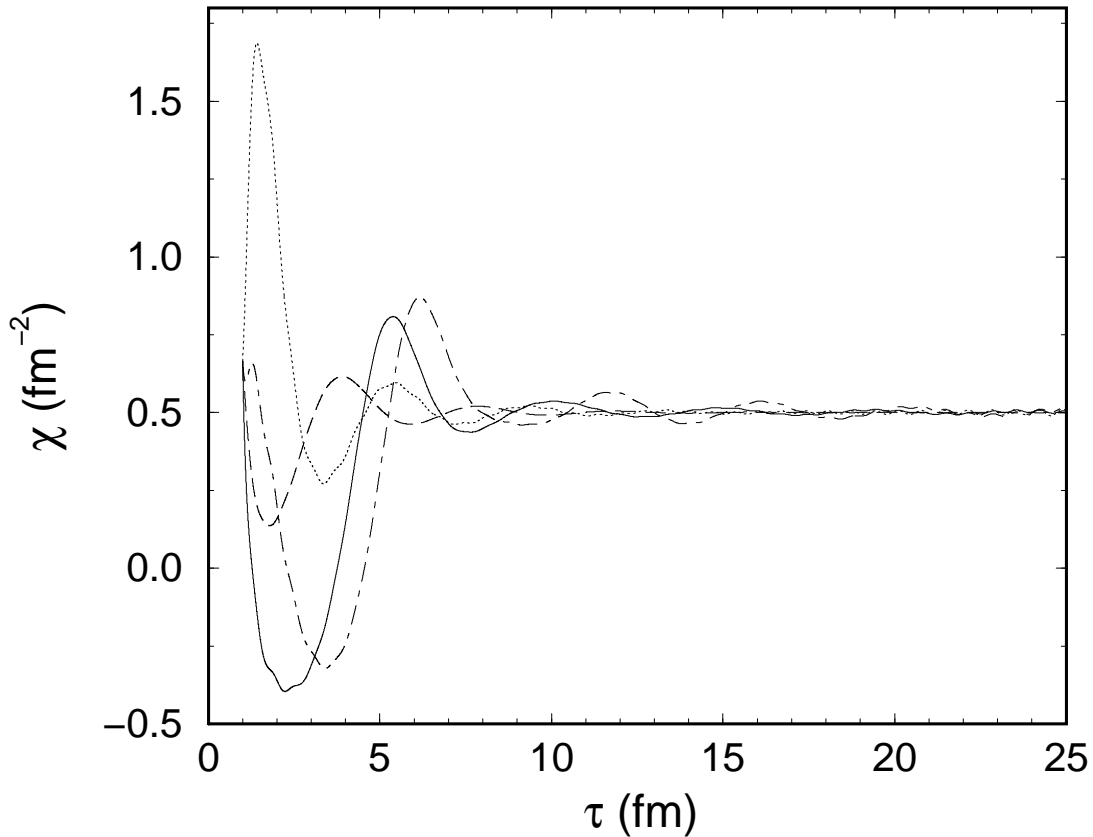


FIG. 1. Proper time evolution of the  $\chi$  field for the following initial conditions: Solid line is for  $\sigma(\tau_0) = \sigma_T$ ,  $\pi_i(\tau_0) = 0$ , and  $\dot{\sigma}(\tau_0) = -1$ . Dashed line is for  $\sigma(\tau_0) = \sigma_T$ ,  $\pi_i(\tau_0) = 0$ , and  $\dot{\sigma}(\tau_0) = 1$ . Dotted line is for  $\sigma(\tau_0) = \sigma_T$ ,  $\pi_i(\tau_0) = 0$ , and  $\dot{\sigma}(\tau_0) = 0$ . Dot-dash line is for  $\sigma(\tau_0) = 0$ ,  $\pi_1(\tau_0) = \sigma_T$ , and  $\dot{\sigma}(\tau_0) = -1$ . At  $T = 200$  MeV,  $\sigma_T = 0.3 \text{ fm}^{-1}$ .

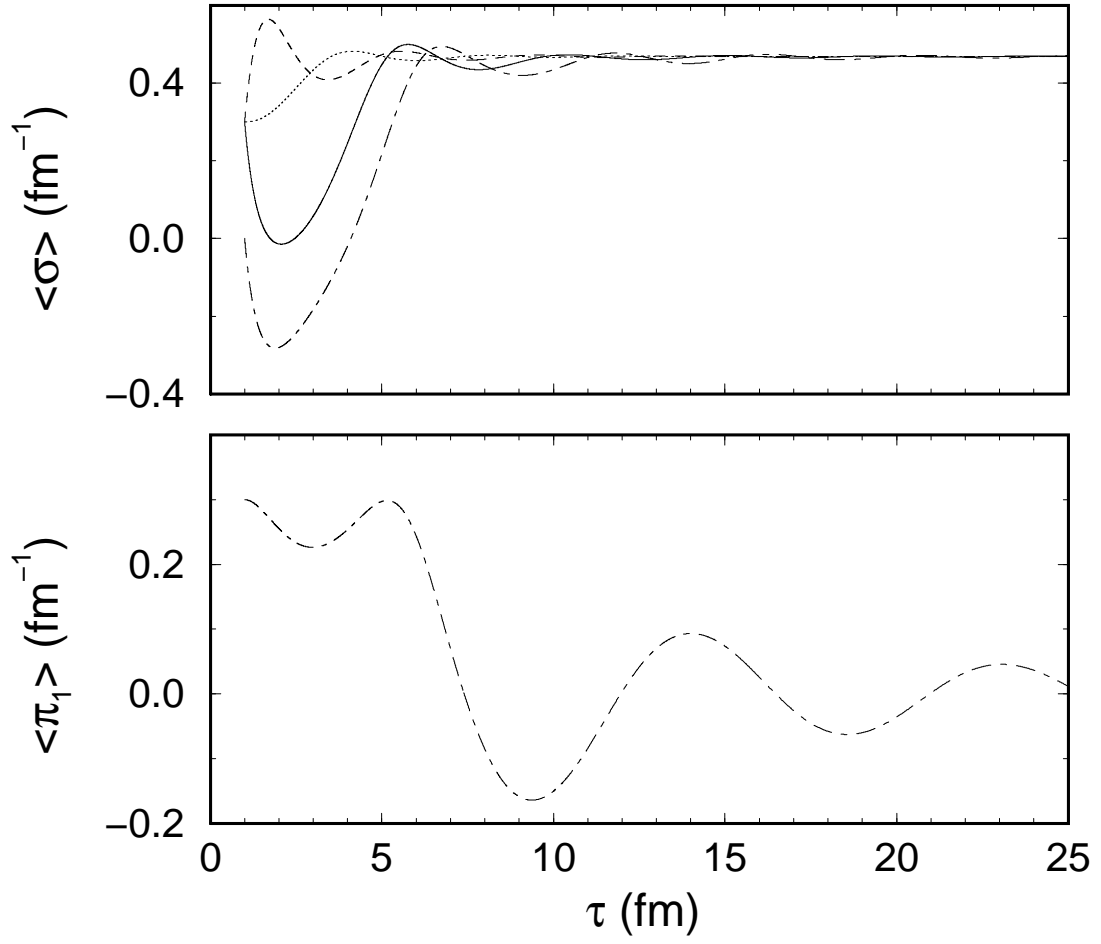


FIG. 2. Proper time evolution of the  $\langle \sigma \rangle$  and  $\langle \pi_1 \rangle$  fields for the same initial conditions as Fig. 1.

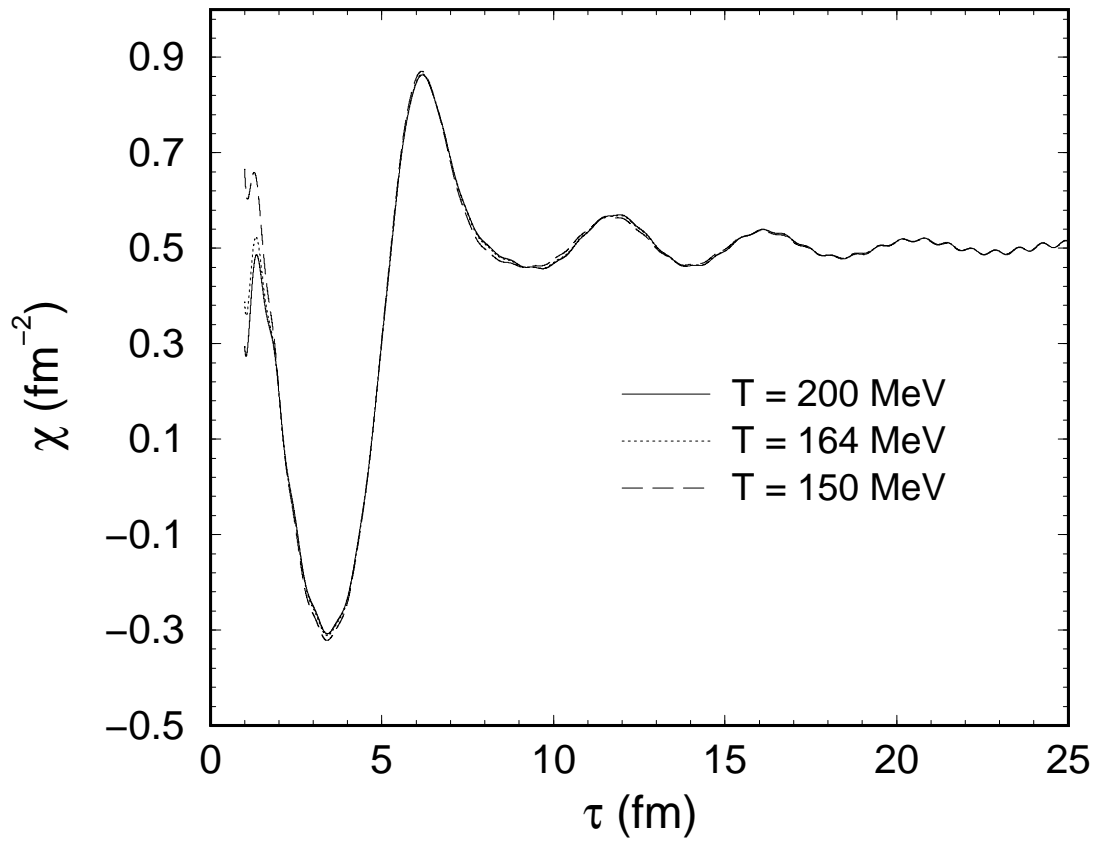


FIG. 3. Proper time evolution of the  $\chi$  field for three different initial thermal distributions with  $T = 200, 164, 150$  MeV for the initial conditions  $\sigma(\tau_0) = \sigma_T$ ,  $\pi_i(\tau_0) = 0$ , and  $\dot{\sigma}(\tau_0) = -1$ .

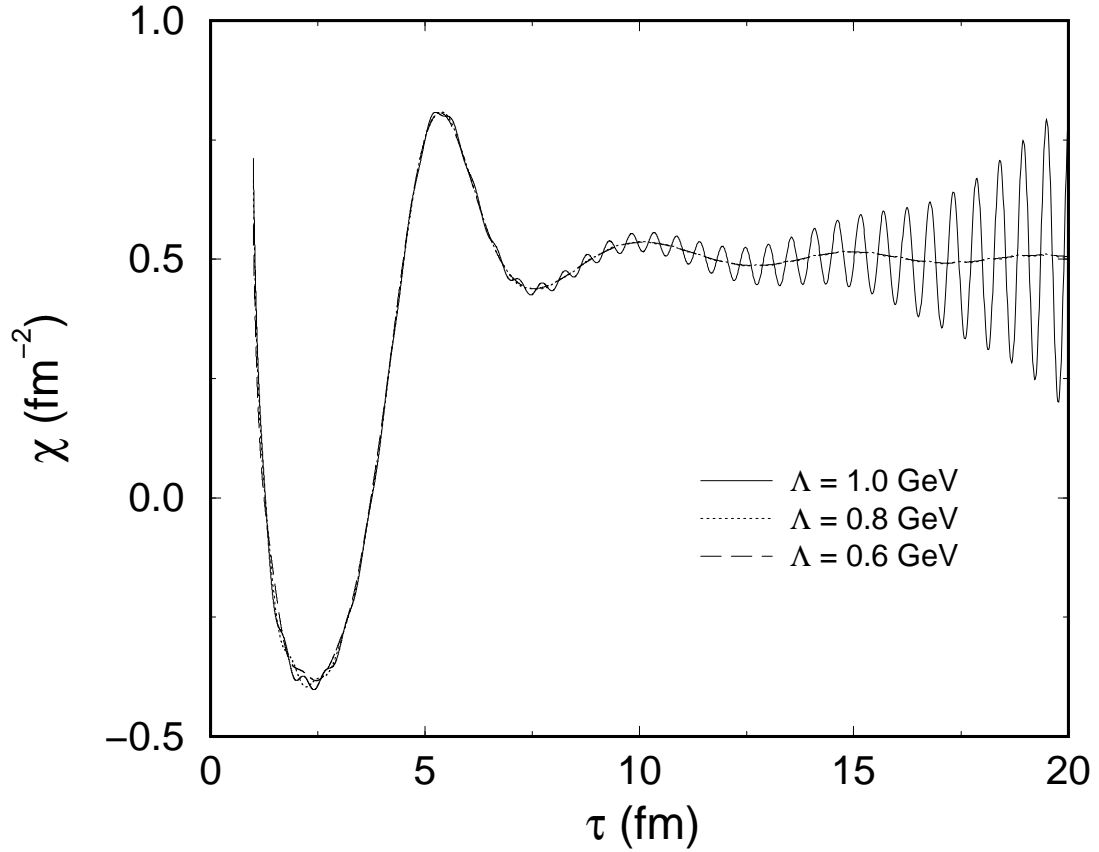


FIG. 4. Proper time evolution of the  $\chi$  field for three different values of the cutoff  $\Lambda$ , with  $\Lambda = 600, 800, 1000$  MeV for the initial conditions  $\sigma(\tau_0) = \sigma_T$ ,  $\pi_i(\tau_0) = 0$ , and  $\dot{\sigma}(\tau_0) = -1$ .

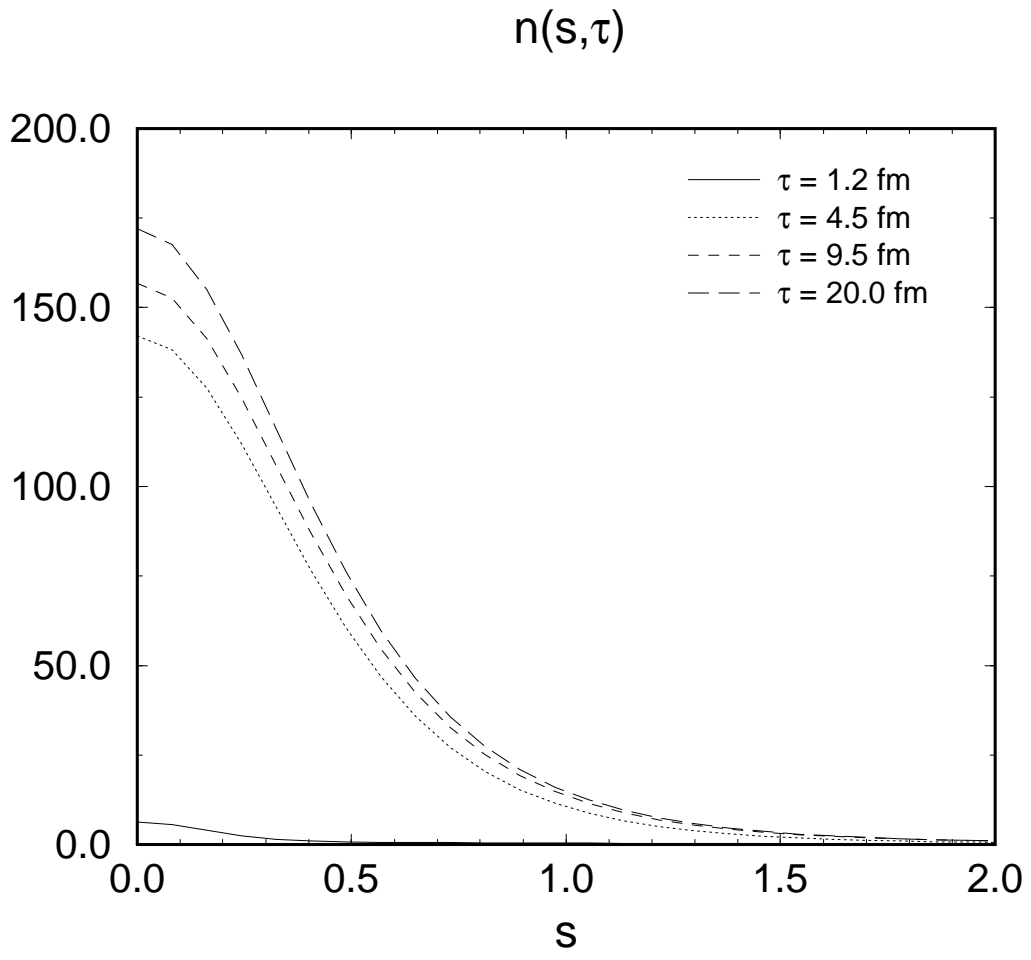


FIG. 5.  $n_s(\tau)$  computed from (3.20), for the initial conditions  $\sigma(\tau_0) = \sigma_T$ ,  $\pi_i(\tau_0) = 0$ , and  $\dot{\sigma}(\tau_0) = -1$ .

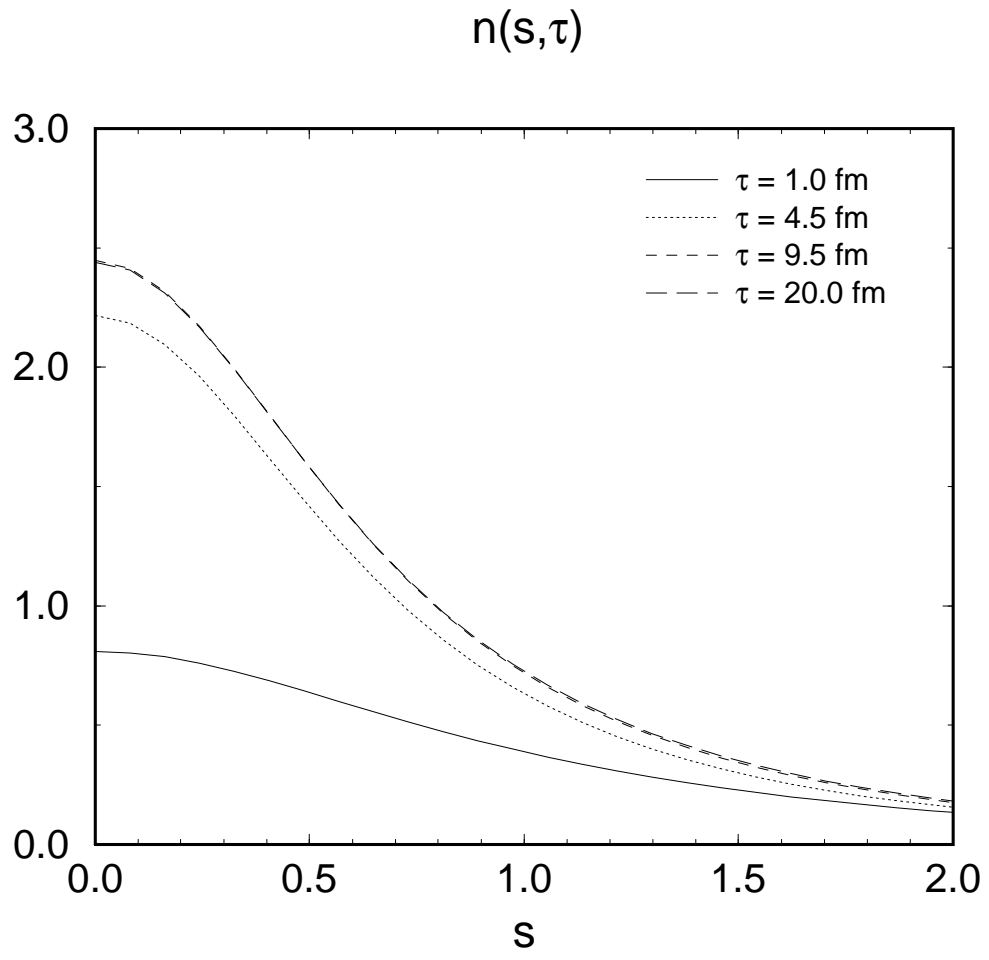


FIG. 6. Same as the previous figure, but for the initial conditions  $\sigma(\tau_0) = \sigma_T$ ,  $\pi_i(\tau_0) = 0$ , and  $\dot{\sigma}(\tau_0) = 0$ .

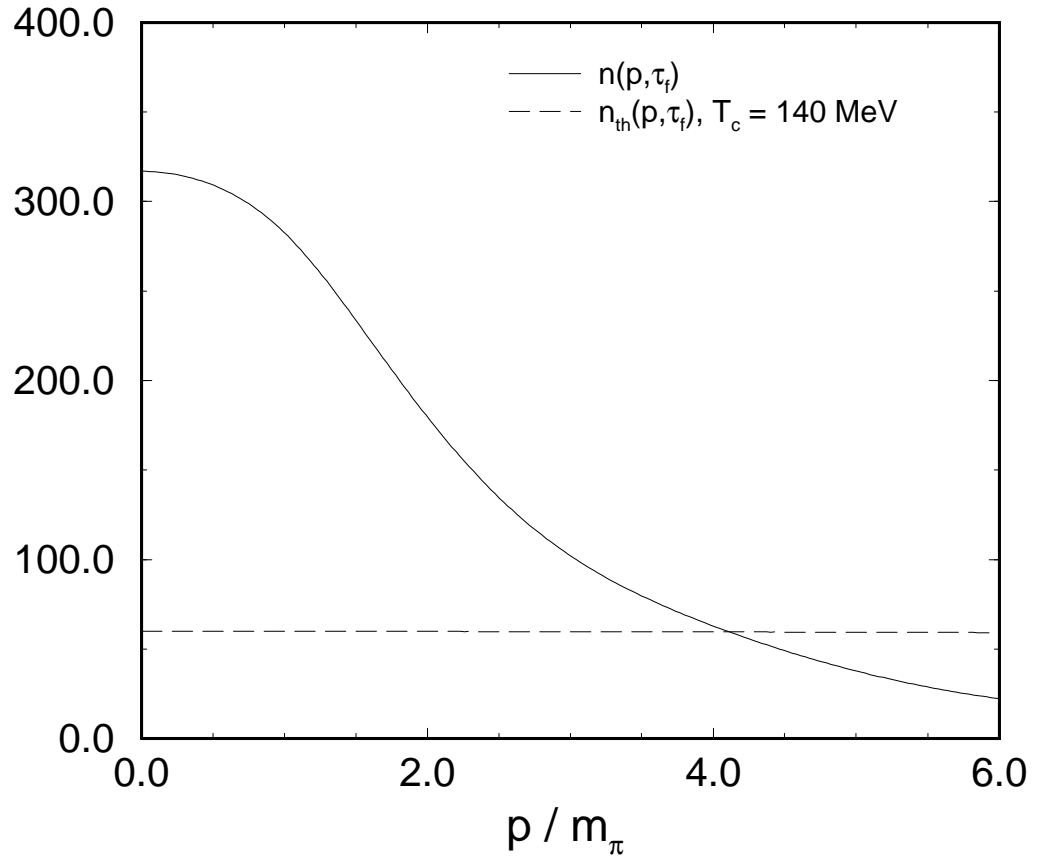


FIG. 7.  $n(p, \tau)$  computed from (B2) and  $n_{th}(p, \tau)$  computed from (B3), for the same initial conditions as Fig. 5.

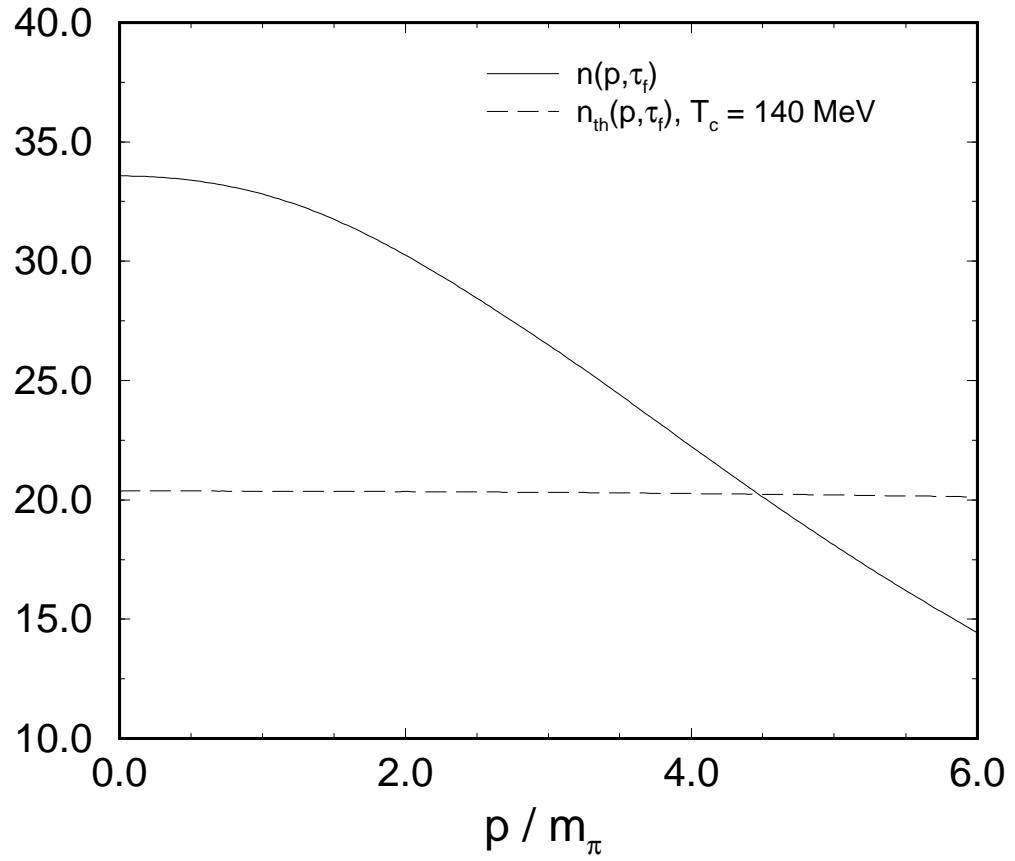


FIG. 8. Same as the previous figure, but for the same initial conditions as Fig. 6.